Polyhedron 28 (2009) 2503–2509

Contents lists available at ScienceDirect

Polyhedron

journal homepage: www.elsevier.com/locate/poly

Intramolecular amide → imine reduction in higher valent rhenium complexes stabilized by arylimido coligand: Rate studies and effect of reductants

Jaydip Gangopadhyay [a,*], Suparna Banerjee [b], Jiu-Tong Chen [c], Can-Zhong Lu [c]

[a] Department of Chemistry, St. Paul's C.M. College, University of Calcutta, 33/1 Raja Rammohan Roy Sarani, Kolkata 700009, India
[b] Department of Chemistry, Uluberia College, University of Calcutta, Howrah 711315, India
[c] The State Key Laboratory of Structural Chemistry, Fujian Institute of Research on the Structure of Matter, The Chinese Academy of Sciences, Suzhou, Fujian 350002, PR China

ARTICLE INFO

Article history:
Received 12 February 2009
Accepted 30 April 2009
Available online 8 May 2009

Keywords:
Amide complex
Outward OAT
Reduction
Imine derivative
Kinetics

ABSTRACT

The present work deals with the imidorhenium(V) complexes of type $[ReCl_3(NC_6H_4Y\text{-}p)(L)]$, with Y = OCH_3(**1d**), CH_3(**1c**), H(**1b**), Cl(**1a**) where L is the pyridylimine Schiff base ligand obtained from facile condensation of pyridine-2-carboxaldehyde and *p*-phenylenediamine. Structural authentication of one representative (**1d**) reveals meridional disposition of three Cl atoms around the metal center in a distorted octahedral $ReCl_3N_3$ coordination environment. $Re\text{–}N^{pyridine}$ bond lying trans to $Re{\equiv}NC_6H_4Y\text{-}p$ motif is lengthened by ~0.2 Å compared to $Re\text{–}N^{imine}$ bond and is attributed to *trans* influence of imide nitrogen. The complexes, **1** are reactive towards dilute aqueous nitric acid furnishing amide bound hexavalent rhenium complexes, **2**. Six lines EPR spectra have been recorded for **2** in solution phase at ambient condition ($g_{iso} \sim 1.945$, $A_{av} \sim 493$ G) and magnetic susceptibility measurement indicates strong orbital coupling consistent with one electron paramagnetic nature (~1.45 μ_B). Re^{VI}/Re^{V} responses for **1** appear at higher potential (~0.95 V) that those observed for **2** (~0.12 V). Type **2** complexes are reduced (low Re^{VI}/Re^{V} reduction potential, +0.15 V) by $N_2H_5^+$ and NH_3OH^+ species under mild condition to regenerate **1**. The reduction with $N_2H_5^+$ is nearly five times faster than NH_3OH^+. Rate study suggests an associative pathway ($\Delta H^{\neq} = 11.61$ kcal mol^{-1}, $\Delta S^{\neq} = -31.22$ eu using $N_2H_5^+$ and $\Delta H^{\neq} = 10.74$ kcal mol^{-1}, $\Delta S^{\neq} = -37.30$ eu using NH_3OH^+) for amide → imine transformation. No such analogous amide → imine conversion has yet been achieved in metal free environment, accentuating the exclusive electronic role of variable metal valence. Further, the oxo complex, **6** does not exhibit intramolecular ligand oxidation suggesting decisive electronic role of the coligands (oxo/arylimido) in stabilizing higher metal valence.

1. Introduction

Higher valent rhenium complexes have spurred interest owing to active participation as catalysts in various molecular transformations featuring key changes like functionality conversion [1], derivatization [2], cyclisation [3,4], oxygen atom transfer [5–7] in the products. Most of the oxygen atom transfer reactions between organic molecules characterizing the red-ox functional pairs like sulphide–sulphoxide; sulphoxide–sulphone; phosphine–phosphine oxide do not proceed at reasonable rates at normal temperature even recognized as thermodynamically favourable. To overcome the kinetic sluggishness, middle and late transition metals multiply bonded to heteroatom coligands have long been successfully employed [8–10] for oxidation of small molecules. Metal bound oxo → dioxo, phosphine → phosphine oxide transformations and metal catalysed sulphide → sulphoxide; pyridine oxide → pyridine; phosphine → phosphine oxide conversions mediated through oxygen atom transfer phenomenon have been authenticated in rhenium chemistry [11–21]. Moreover, abiological molecular oxotransferase incorporating $Re^{V}O$ motif has been established as useful catalyst to successfully accomplish reductions of stable inorganic moieties like ClO_4^-, NO_3^-, NO [22].

Structure-reactivity correlation reveals the prevalence of multiply bonded oxo (O^{2-}) coligand to the higher valent metal in the promising catalysts. Our programme focuses on the study of redox related organic functionality pair conversion assisted by imido (NR^{2-}) bonded higher valent rhenium complexes. Herein, we report ligand centered oxygen atom abstraction followed by reduction providing access to route of

* Corresponding author.
E-mail address: gjaydip@rediffmail.com (J. Gangopadhyay).

0277-5387/$ - see front matter © 2009 Elsevier Ltd. All rights reserved.
doi:10.1016/j.poly.2009.04.040

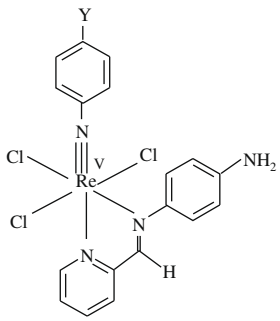

1

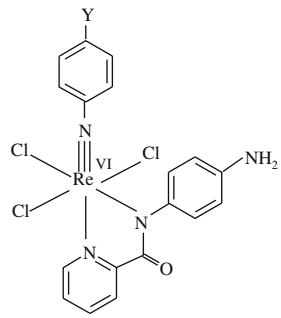

2

facile amide → imine conversion in secondary metal coordination sphere. The amide chelated imidorhenium(VI) complexes (**2**) were prepared by oxidation of imine bound imidorhenium(V) complexes (**1**) with dilute HNO_3. Complexes of type **2**, on reaction with either $N_2H_5^+$ or NH_3OH^+ undergoes outward oxygen atom transfer and reduced to the imine complex **1**. This observation is unprecedented in the sense of mobilizing a metal bound amide function (most inactive carboxylic acid derivative) to participate in electronic and geometrical changes resulting in the generation of reduced imine form.

The syntheses, representative structure determination of **1**, metal redox and spectroscopic properties of complexes are reported. The kinetic behaviour of outward oxygen atom transfer has been studied and a viable mechanism consistent with the experimental findings and kinetics is proposed.

2. Results and discussion

2.1. Synthesis

Facile condensation of pyridine-2-carboxaldehyde and *p*-phenylenediamine in a 1:1 molar ratio respectively, afforded a neutral condensate, N-p-aminophenyl-2-pyridinecarboxaldimine **L**, which has been employed as a bidentate ligand in the present

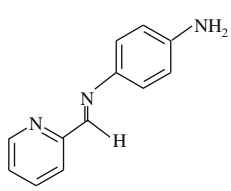

L, $C_{12}H_{11}N_3$

work. The violet coloured complexes **1**, $[Re(NC_6H_4Y\text{-}p)Cl_3L]$ (Y = Cl(**1a**), H(**1b**), CH_3(**1c**), OCH_3(**1d**)) are formed in good yields upon reacting $[Re(NC_6H_4Y\text{-}p)Cl_3(PPh_3)_2]$ with L in 1:1.5 molar ratio in benzene under reflux followed by chromatographic work up of the reaction mixture. In the product, two *trans* oriented PPh_3 groups are being substituted by the ligand L, Eq. (1).

$$[Re^{V}(NC_6H_4Y)Cl_3(PPh_3)_2] + L \rightarrow [Re^{V}(NC_6H_4Y)Cl_3(L)] + 2PPh_3 \quad (1)$$

1 reacts smoothly with aqueous nitric acid [23] in acetonitrile solution at room temperature under stirring condition resulting yellow picolinamide complexe (**2**). The feasibility of the reverse reaction **2** → **1** has been scrutinized with different reducing agents and successfully carried out using nitrogenous reagents like hydrazine sulphate (Eq. (2)) and hydroxylamine hydrochloride (Eq. (3)) at mild condition in acetonitrile medium.

$$[Re^{VI}(NC_6H_4Y)Cl_3(C_{12}H_{10}N_3O)] + 3N_2H_5^+ \rightarrow [Re^{V}(NC_6H_4Y)Cl_3(C_{12}H_{11}N_3)] + \frac{3}{2}N_2 + 3NH_4^+ + H_2O \quad (2)$$

$$4[Re^{VI}(NC_6H_4Y)Cl_3(C_{12}H_{10}N_3O)] + 6NH_3OH^+ \rightarrow 4[Re^{V}(NC_6H_4Y)Cl_3(C_{12}H_{11}N_3)] + 3N_2O + 6H^+ + 7H_2O \quad (3)$$

2.2. Magnetic moment, NMR and EPR spectra

The type **1** complexes are diamagnetic corresponding to low spin $5d^2$ electronic configuration and the effective magnetic moment data of complexes **2** confirm the presence of one unpaired electron ($5d^1$, $s = 1/2$) in a pseudo-octahedral environment although the magnetic moments are significantly lower (**2a**, 1.42 μ_B; **2b**, 1.45 μ_B; **2c**, 1.46 μ_B; **2d**, 1.47 μ_B) than the spin only value. The lowering could be attributed to appreciable orbital coupling [24] as encountered in other hexavalent rhenium species.

The type **1** complexes uniformly exhibit well separated NMR signals in solution consistent with diamagnetism. However, amide complexe (**2**) display paramagnetically shifted relatively broad peaks lacking well resolved spin-spin structures. The type **2** complexes are EPR active (Fig. 1, Table 1) in fluid solution at room temperature and display well resolved spectra consisting of six isotropic hyperfine lines due to the interaction of the unpaired electron with the nuclear spin of both rhenium isotopes ($I = 5/2$; ^{185}Re, 37.07%; ^{187}Re, 62.93%). The isotopic fine structure has not been resolved because of the small difference (1%) in the two nuclear quadrupole moments. There is a systematic increase in the separation between the adjacent hyperfine lines on going from lower to higher fields due to the second order effects [25]. The range of this variable hyperfine

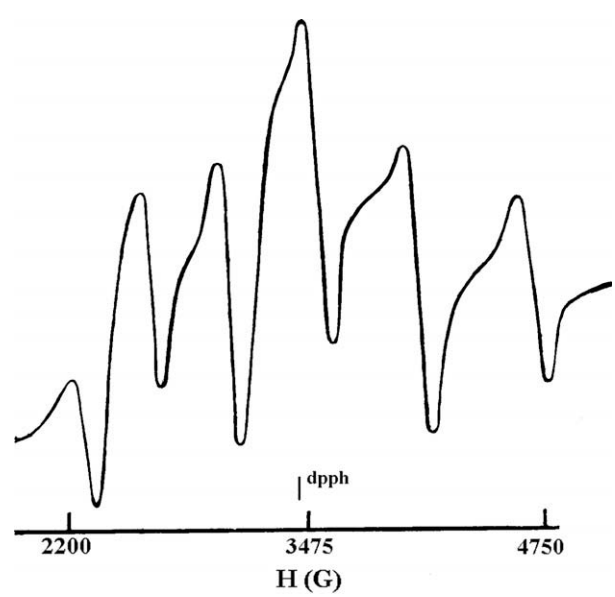

Fig. 1. EPR diagram of Complex **1d** in solution phase at 9.1 GHz and 298 K.

Table 1
EPR data for **2** at 298 K in dichloromethane-benzene (1:1) solution.

Complexes	Center field g	A (G, average)
2a	1.939	488
2b	1.945	492
2c	1.948	498
2d	1.957	496

spacing spans the domain 360-640 G, consistent with very high oxidation state (+VI) of the metal. Centre field g values and average hyperfine splitting A for the complexes fall in the ranges 1.939–1.957 and 488–498 G, respectively. Well resolved sextet EPR spectra in solution at ambient temperature are relatively rare for Re(VI) owing to the comparatively large line width followed by significant overlapping and only broad signals [26–28] are usually observed. However, Re(VI) complexes of type $[ReNX_4]^-$ (X = Cl, Br and NCS) follow similar spectral characteristics [29] at room temperature.

The spectra of **2** in a frozen (77 K) dichloromethane/toluene glass become axial and are characterized with individual g-tensors ~1.92 ($g_{||}$) and ~1.98 ($g_{\perp}$). The observed g inequality is consistent with a tetragonally distorted octahedral geometry. The hyperfine components due to the $g_{||}$ resonance (reference axis, Re≡NAr), especially the outer components have been resolved to a satisfactory extent whereas the components corresponding to $g_{\perp}$ absorptions overlap considerably. This observation corroborates that the rhombic field is not strong enough to split the perpendicular absorption into individual tensors (g_{xx} and g_{yy}). The separations between $g_{||}$ hyperfine lines are unequal and gradually increases towards higher field. It is noteworthy that the separations between $g_{||}$ hyperfine structures are larger (350–800 G) than those in isotropic solution (360–640 G) and the inter spacing between $g_{\perp}$ components are correspondingly smaller.

2.3. UV–visible and IR spectra

The electronic spectra for type **1** and **2** complexes were recorded in dichloromethane solution at room temperature. The Re^V chelates (**1**) display a relatively weak transition near 750 nm related to $5d_{xy} \rightarrow d_{yz}, d_{xz}$ excitation. Well separated moderately intense second band appeared at about 540 nm, presumably LMCT ($\pi_{Cl} \rightarrow Re^V$) in origin. Another highly intense band near 350 nm could be ascribed to bound aldimine based internal CT transition. Spectra of **2** are characterized with two peaks in higher energy (535 and 350 nm) and disappearance of lowest energy peak.

All IR spectra of **1** and **2** exhibit two primary N–H stretching modes near 3350 and 3280 cm^{-1} as sharp doublets for the asymmetric and symmetric vibrations, respectively. The strong bands observed in the range 1590–1610 cm^{-1} are assigned to C=N stretch and red shift of this azomethine absorption by ~25 cm^{-1} from free ligand to the complexes suggests weak π–accepting property of the coordinated ligand. Two Re–Cl stretches were observed in the region 320–340 cm^{-1}, consistent with *mer*-$ReCl_3$ motif for both types of complexes. Picolinamide bound complexes (**2**) uniformly exhibit another characteristic band near 1640 cm^{-1} for C=O function of the ligand.

2.4. Structure

The X-ray structure of **1d** has been determined. Molecular view, atom numbering scheme are presented in Fig. 2 and selected bond parameters are collected in Table 2.

The $ReCl_3$ fragment is uniformly disposed in a meridional fashion in the distorted octahedral complex. The Cl1, Cl2, Cl3 and N2 atoms define a good equatorial plane (mean deviation ~0.01 Å) from which the metal atom is displaced towards the imide nitrogen N4 by 0.30 Å. The five membered chelate ring (Re, N1, C5, C6 and N2) along with the pyridine moiety constitute a satisfactory plane (md < 0.02 Å) with which the p-aminophenyl group of the ligand L is obliquely oriented (dihedral angle ~70°). Trans influence of imido nitrogen (N4) is reflected in the Re–N1 bond length (2.236 Å), longer by about 0.19 Å compared to normal Re–N2 length (2.045 Å). The Re–N4 length, 1.714(3) Å and Re–N4–C13 angle, 173.9(2)° are consistent with the triply bonded ($\sigma^2\ \pi^4$), more or less linear arylimidorhenium (Re^V≡NC_6H_4Y) motif [30,31].

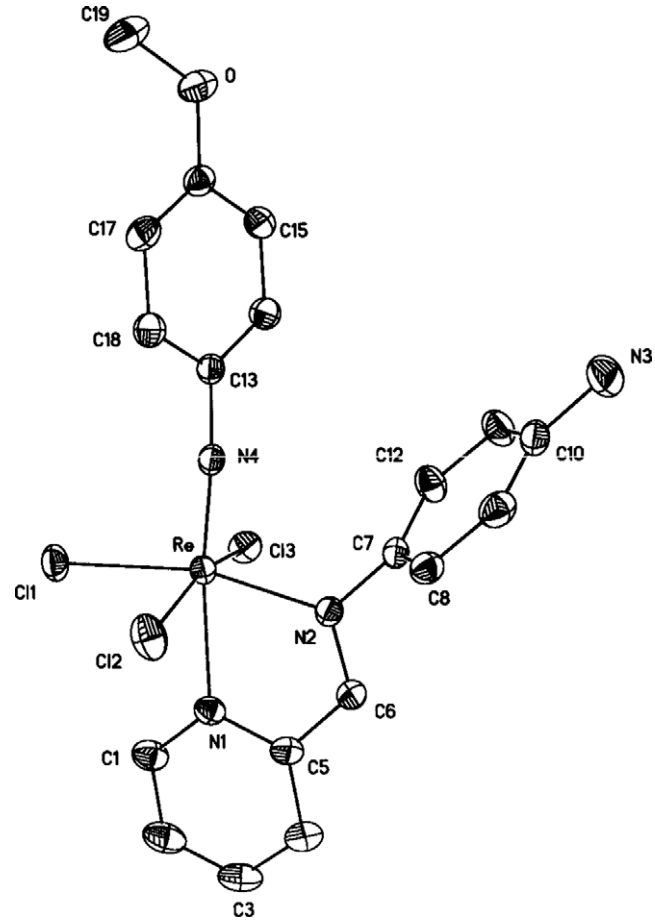

Fig. 2. A perspective view (25% probability thermal ellipsoids) and atom labeling scheme of **1d**. Hydrogen atoms have been omitted for clarity.

Table 2
Selected bond distances (Å) and angles (°) for **1d**.

Distances			
Re–N(4)	1.714(3)	Re–N(2)	2.045(2)
Re–N(1)	2.236(3)	Re–Cl(2)	2.3813(10)
Re–Cl(1)	2.3826(9)	Re–Cl(3)	2.3856(9)
Angles			
N(4)–Re–N(2)	98.63(11)	N(4)–Re–N(1)	173.01(10)
N(2)–Re–N(1)	74.85(10)	N(4)–Re–Cl(2)	99.72(9)
N(2)–Re–Cl(2)	87.34(7)	N(1)–Re–Cl(2)	82.69(7)
N(4)–Re–Cl(1)	96.51(8)	N(2)–Re–Cl(1)	164.81(7)
N(1)–Re–Cl(1)	90.09(7)	Cl(2)–Re–Cl(1)	88.83(4)
N(4)–Re–Cl(3)	95.56(9)	N(2)–Re–Cl(3)	91.71(7)
N(1)–Re–Cl(3)	82.29(7)	Cl(2)–Re–Cl(3)	164.66(4)
Cl(1)–Re–Cl(3)	88.12(3)		

Molecular packing reveals that one Cl atom of a molecule underwent two weak Cl···H contacts (2.829 and 2.898 Å) with two other proton donor molecules oriented in a nearly parallel manner to the acceptor. The donor fragments are linked through O···H interaction (2.461 Å) to form a trimeric assembly and the pattern is extended inside the lattice. Apart from the said interactions, the stability of the trimer is partly imparted from π–π stacking force operating between arylimido and aminophenyl groups (centroid···centroid distance – 3.885 Å) of two donor molecules.

2.5. Electrochemistry

All the two families are electroactive in acetonitrile solution at platinum electrode. The reduction potential data are collected in

Table 3
Cyclic voltammetric formal potentials at 298 K in acetonitrile solvent (TEAP, supporting electrolyte) at a platinum working electrode.[a,b,c,d]

Complex **1**	$E_{½}$ (Re^{VI}/Re^{V}),V (ΔE_p, mV)	Complex **2**	$E_{½}$,V (ΔE_p, mV)	
			Re^{VI}/Re^{V}	Re^{VII}/Re^{VI}
1a	1.02 (80)	**2a**	0.16(80)	1.58(80)
1b	0.97(85)	**2b**	0.13(80)	1.54(85)
1c	0.95(80)	**2c**	0.11(85)	1.52(85)
1d	0.91(80)	**2d**	0.08(80)	1.48(80)

[a] Scan rate 50 mVs^{-1}.
[b] $E_{½} = ½ (E_{pa} + E_{pc})$, where E_{pa} and E_{pc} are anodic and cathodic peak potentials, respectively.
[c] $\Delta E_p = E_{pa} - E_{pc}$.
[d] Reference electrode SCE.

Table 4
Rate constants and activation parameters[a] for the conversion **2**→**1** in acetonitrile using $[N_2H_5^+]$.[b,c]

T (K)	$[N_2H_5^+]$, M	10^3 k_{obsd}, s^{-1}	10^3k_2, $M^{-1}s^{-1}$
299	1.11	2.84	2.63(0.02)
	1.67	4.33	
	2.22	5.74	
296	1.11	2.30	2.13(0.03)
	1.67	3.49	
	2.22	4.68	
293	1.11	2.04	1.77(0.04)
	1.67	3.06	
	2.22	4.02	
288	1.11	1.19	1.21(0.04)
	1.67	1.88	
	2.22	2.54	
283	1.11	0.72	0.82(0.03)
	1.67	1.21	
	2.22	1.64	

[a] $\Delta H^{\neq}$ = 11.61 (0.59) kcal mol^{-1} and $\Delta S^{\neq}$ = −31.22 (2.4) eu.
[b] The initial concentration of **2** is 2.5×10^{-4} M.
[c] Least squares deviations are given in parentheses.

Table 5
Rate constants and and Activation parameters[a] for the conversion **2**→**1** in acetonitrile using $[NH_3OH^+]$.[b,c]

T (K)	$[NH_3OH^+]$, M	10^3 k_{obsd}, s^{-1}	10^3k_2, $M^{-1}s^{-1}$
299	1.11	0.54	0.53(0.04)
	1.67	0.89	
	2.22	1.13	
296	1.11	0.50	0.44(0.03)
	1.67	0.71	
	2.22	0.99	
293	1.11	0.42	0.37(0.01)
	1.67	0.61	
	2.22	0.83	
288	1.11	0.25	0.26(0.02)
	1.67	0.37	
	2.22	0.54	
283	1.11	0.15	0.18(0.03)
	1.67	0.24	
	2.22	0.35	

[a] $\Delta H^{\neq}$ = 10.74 (0.62) kcal mol^{-1} and $\Delta S^{\neq}$ = −37.30 (2.1) eu.
[b] The initial concentration of **2** is 2.5×10^{-4} M.
[c] Least squares deviations are given in parentheses.

Table 3. The type **1** complexes display well-defined quasi-reversible anodic peak (peak to peak separation ~ 80 mV) near 0.95 V versus SCE. The response is tentatively assigned to the oxidation of Re^{V} to Re^{VI} and relevant to the redox reaction $\mathbf{1^+} + e \rightarrow \mathbf{1}$. The potential increases with the increase in electron withdrawing power of Y (OCH_3 < CH_3 < H < Cl) and the observed trend follows usual Hammett order. The picolinamide complexes of type **2** exhibit two successive quasi-reversible (peak to peak separation ~ 80 mV) one electron signals near 0.15 and 1.50 V for Re(VI)/Re(V) and Re(VII)/Re(VI) couples respectively (Eq. (4)).

$$\mathbf{2} + \mathbf{e} \rightarrow \mathbf{2^-} \quad (4a)$$

$$\mathbf{2^+} + \mathbf{e} \rightarrow \mathbf{2} \quad (4b)$$

Lowering of reduction potential for Re^{VI}/Re^{V} couple by a substantial margin of ~0.8 V for type **2** complexes compared to that of **1** indicates superior stabilization of amide bound hexavalent rhenium in the former species [32]. Like **1**, type **2** complexes also exhibit substitution effect at Y of arylimido moiety in a usual manner.

2.6. Reduction kinetics

In order to understand the kinetic behaviour of amide → imine reduction, the progress of the reaction was monitored by spectrophotometry in acetonitrile solution. The conversion **2** → **1** was characterized by the increase in absorbance at 535 nm in the temperature interval 283–299 K. The second order rate constants at different temperatures and activation parameters for the reaction using $N_2H_5^+$ are collected in Table 4. Under pseudo-first order condition (excess hydrazine), the rates are found to be proportional to the concentration of amide complex **2** (Rate = k_{obsd} [2]), as evident from the linear plots of $-\ln(A_\alpha - A_t)$ versus time t at different hydrazine concentrations under variable temperatures. The plot between any set of k_{obsd} values and used hydrazine concentrations at any recorded temperature is linear in nature and the corresponding slope gives the second order rate constant k_2 as stated in Eq. (5). First order dependence of **2** and

$$\text{Rate} = k_2[\mathbf{2}][\mathbf{N_2H_5^+}](\mathbf{k_{obsd}} = \mathbf{k_2}[\mathbf{N_2H_5^+}]) \quad (5)$$

hydrazine on rate implies that the oxygen atom transfer reaction proceeds through the rate determining step involving close association ($\Delta S^{\neq}$ = −31.22 eu) of hexavalent metal amide substrate and the reducing agent.

The rate of reduction of **2** by $N_2H_5^+$ was found to be nearly five times faster than that measured with NH_3OH^+ (Table 5) at all recorded temperatures. The difference in rates can be reconciled by considering higher reducing ability of $N_2H_5^+$ (higher oxidation potential) over NH_3OH^+ (lower oxidation potential).

2.7. Reaction model

N_2H_4 has the unique ability to act as either one electron or multi electron (two and four) donor reducing agent depending on the reaction condition and nature of the oxidant. The number of proton and electron equivalents transferred from each equivalent of $N_2H_5^+$ is a requisite for the proposition of reduction mechanism. Isolation of ammonium salt from the products of **2** → **1** conversion is consistent with one electron and one proton donor function of $N_2H_5^+$, relevant to half cell reaction, $N_2H_5^+ \rightarrow ½N_2 + NH_4^+ + H^+ + e$.

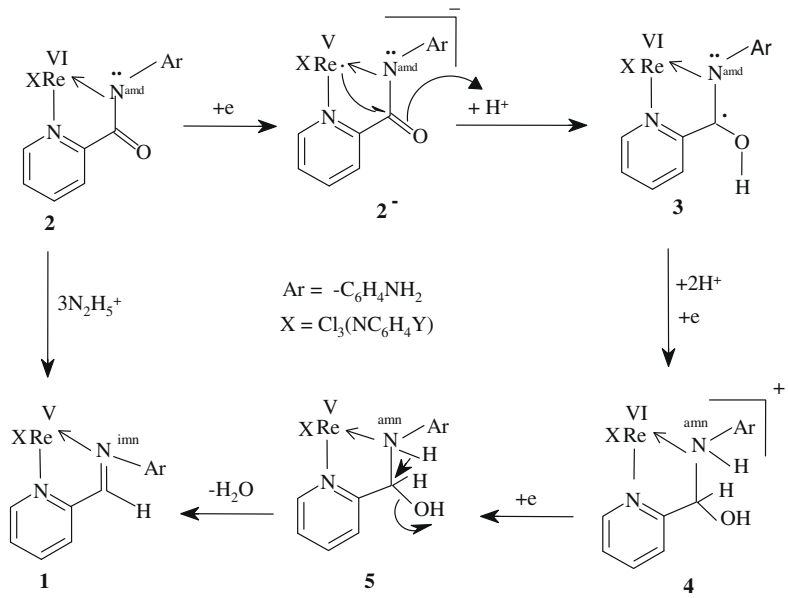

Scheme 1.

2 → **1** conversion does not involve nucleophilic attack of hydrazine instead outward transfer of oxygen atom from the bonded ligand occurs through proton assisted amide C=O labilisation. In attempt to extend the reaction model (Scheme 1), the initiation is thought to occur via fast metal reduction (low Re^{VI}/Re^{V} reduction potential, ~0.15 V) by $N_2H_5^+$ to form the anionic complex $\mathbf{2}^-$. Lower metal valence (+V) in $\mathbf{2}^-$ considerably decreases the Lewis acidity of the metal and expansion of radius upon reduction substantially weakens Re-amido nitrogen bonding.

These electronic changes in $\mathbf{2}^-$ promote internal electron transfer [33] from pentavalent metal to the amide function and augmented oxygen basicity arising there from induces proton capture [34] to generate the radical based reactive Re(VI) species, **3**. Such electron transfer events are facile in $\mathbf{2}^-$ containing comparatively electron rich Re^{V} centre rather than in **2** incorporating electron poor Re^{VI} metal. Subsequent reduction of amido carbon and nitrogen sites in **3** resulted cationic α-hydroxyamine intermediate, **4** [35–39]. Finally, **4** undergo metal reduction followed by dehydration to regenerate **1**. Elimination of water from **5** is driven by stronger Re^{V}-imine bonding, resulting from metal electron density delocalization over π^* framework of aldimine ligand. The proposed mechanism indicates stepwise utilization of three equivalents of proton and three equivalents of electron derived from three equivalents of $N_2H_5^+$ for the reduction of one equivalent of **2**. This observed reaction stoichiometry is in complete agreement with Eq. (2).

In support of the existence of transient reduced species $\mathbf{2}^-$, we performed constant potential exhaustive reduction of **2** at +0.30 V in dry acetonitrile solvent under deareated condition. The coulomb count ratio suggests an almost quantitative one electron reduction of **2** to form stereoretentive Re^{V} analogue ($\mathbf{2}^-$), evident from the virtually superposable cyclic voltammogram of the electrogenerated species $\mathbf{2}^-$ (anodic scan) with that of **2** (cathodic scan). Attempts to isolate $\mathbf{2}^-$ did not succeed. Such an analogous transformation of N-substituted amide to imine has not yet been documented in metal free condition. Appreciable π-delocalisation in free amide makes amido oxygen feebly basic hindering the protonation step and no scope for induced electron transfer halts the successive stages of the transformation. Hence, the concerned **2** → **1** conversion is entirely metal regulated in electronic sense via easy accession of variable metal valence as required in different steps.

2.8. Coligand effect on intramolecular oxidation

π-acidic Re^{V} ion can be stabilized with the help of π-donor oxo and arylimido coligands. The scrutiny of imine → amide conversion in the Re^{V}-oxo complex (**6**), $[Re^{V}OCl_3L]$ can help us to understand role of electronic effect of coligands exerted on oxidation process. With the aim to investigate, we prepared the concerned oxo complex and allowed to react with aqueous HNO_3 under the same condition. The reaction was only ended up with no observable colour change and no isolation of the corresponding amide product. The observation implies that the Re^{VI} ion is better stabilized by arylimido

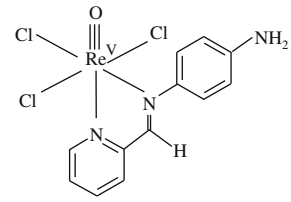

6

group compared to the oxo coligand. This is attributed to superior π-donor ability of arylimido group (NAr^{2-}) over oxo (O^{2-}) to efficiently stabilize the Re^{VI} centre as attested from the higher oxidation potential of oxo complex, **6** (1.55 V) than the imido complexes, **1** (~0.95 V) and the lower electronegativity of nitrogen than oxygen. Significantly high oxidation potential for the oxo complex renders the rhenium metal inactive for initial oxidation to promote imine → amide oxidation. Moreover, coulometric oxidation of $[Re^{V}OCl_3L]$ in dry acetonitrile solvent afforded no tractable Re^{VI} product which suggests that the Re^{VI} analogue is only stable in cyclic voltammetric short time scale.

3. Conclusion

Reported pyridylimine chelated type **1** imidorhenium(V) complexes are active towards inward oxygen atom transfer reaction in dilute nitric acid medium affording pyridylamide bound hexavalent rhenium analogues, **2**. Low Re^{VI}/Re^{V} potential for **2** provides the opportunity to scrutiny the reductive susceptibility with nitroge-

nous reducing agents like hydrazine sulphate and hydroxylamine hydrochloride. Rate measurements for **2**→**1** conversion reveal an associative pathway and on that basis reaction mechanism is proposed. The reduction mode explains the role of variable metal valence in proton mediated structural changes of the bound amide ligand in **2**. The oxo complex (**6**) does not respond to such imine→amide oxidation owing to considerably high metal oxidation potential.

Electroactive complexes of type **2** display Re^{VI}/Re^{V} and Re^{VII}/Re^{VI} voltammetric signals near ~0.1 and ~1.6 V in contrast to only one Re^{VI}/Re^{V} couple (~0.95 V) for **1**. The appearance of Re^{VII}/Re^{VI} response for **2** implies superior stabilizing effect of amide group for higher valent rhenium species. Type **2** complexes uniformly exhibit one electron paramagnetism and display well-resolved six lines EPR spectra at room temperature in solution.

4. Experimental

4.1. Materials and physical measurements

The starting materials $[Re(NC_6H_4Y)Cl_3(PPh_3)_2]$ [40] and $[ReOCl_3(PPh_3)_2]$ [41] and the ligand L [42] were synthesized by reported standard methods. All other chemicals were of reagent grade and used as received. Solvents were dried and distilled prior to use. The IR spectra were recorded on KBr pellets with a Perkin–Elmer FT-IR spectrometer. A Perkin–Elmer 2400 II elemental analyzer was used for microanalysis. The electronic spectra and kinetic studies were done using Hitachi U-3501 spectrophotometer fitted with thermostated cell compartments. Electrochemical measurements were performed using a PAR model Versastat-2 electrochemical analyzer, with a platinum working electrode. The supporting electrolyte was tetraethylammonium perchlorate (TEAP), and the potentials were referenced to saturated calomel electrode (SCE) without junction correction. X-band EPR spectra in solution and frozen glass states were recorded using a Bruker 300E spectrometer. Magnetic susceptibilities were measured on a PAR 155 vibrating sample magnetometer.

4.2. Preparation of complexes

4.2.1. Synthesis of $[Re^{V}(NC_6H_4Y)Cl_3(C_{12}H_{11}N_3)]$, **1**

The same general procedure was used to synthesize the above complexes from $[Re^{V}(NC_6H_4Y)Cl_3(PPh_3)_2]$. Procedural details are given for one representative case (**1d**). Yields varied in the range 80–85%.

To a green suspension of $[Re^{V}(NC_6H_4Y)Cl_3(PPh_3)_2]$ (190 mg, 0.20 mmol) in 30 ml of benzene was added 60 mg (0.30 mmol) of L in 10 ml of benzene, and the mixture was heated to reflux for 2 h, affording a violet solution. The solvent was then removed under reduced pressure, and the dark mass thus obtained was subjected to chromatography on a silica gel column (25 × 1 cm, 60–120 mesh). Excess ligand and phosphine was eluted with benzene. A violet band was then eluted with benzene-acetonitrile (20:1) mixture. Solvent removal form the eluate under reduced pressure afforded $[Re^{V}(NC_6H_4OCH_3)Cl_3(L)]$, **1d** as a violet solid. Yield: 106 mg (82%). *Anal.* Calc. for $C_{19}H_{18}Cl_3N_4ORe$: C, 37.35; H, 2.95; N, 9.17. Found: C, 37.30; H, 2.98; N, 9.13. UV–vis (λ_{max}, nm (ε, M^{-1} cm^{-1}), CH_2Cl_2 solution): 735 (1500); 540 (7500); 325 (13200). IR (cm^{-1}): 320, 335 (Re–Cl), 1595 (C=N). ^1H NMR [δ (*J*/Hz), $CDCl_3$ solution]: L, 9.41(H(1), d, 5.5); 6.84 (H(2), t, 7.5); 7.98 (H(3), t, 8.4); 7.34 (H(4), d, 7.7); 6.41(H(6), s); 7.45–7.55 (H(8,9,11,12), m); 16.06 (NH_2, s); $NC_6H_4OCH_3$, 7.08 (2H(o), d, 5.3); 7.13 (2H(m), d, 5.4); 3.99 (OCH_3, s).

1c: *Anal.* Calc. for $C_{19}H_{18}Cl_3N_4Re$: C, 38.35; H, 3.03; N, 9.42. Found: C, 38.31; H, 2.99; N, 9.37. UV–vis (λ_{max}, nm (ε, M^{-1} cm^{-1}), CH_2Cl_2 solution): 735 (1500); 540 (7500); 330 (13400). IR (cm^{-1}): 325, 335 (Re–Cl), 1595 (C=N). ^1H NMR [δ (*J*/Hz), $CDCl_3$ solution]: L, 9.40(H(1), d, 5.5); 6.86 (H(2), t, 7.4); 7.96 (H(3), t, 8.2); 7.33 (H(4), d, 7.3); 6.41(H(6), s); 7.46–7.57 (H(8,9,11,12), m); 16.08 (NH_2, s); $NC_6H_4CH_3$, 7.06 (2H(o), d, 5.5); 7.15 (2H(m), d, 5.4); 4.04 (CH_3, s).

1b: *Anal.* Calc. for $C_{18}H_{16}Cl_3N_4Re$: C, 37.21; H, 2.75; N, 9.65. Found: C, 37.23; H, 2.78; N, 9.63. UV–vis (λ_{max}, nm (ε, M^{-1} cm^{-1}), CH_2Cl_2 solution): 735 (1500); 540 (7500); 325 (13300). IR (cm^{-1}): 320, 335 (Re–Cl), 1600 (C=N). ^1H NMR [δ (*J*/Hz), $CDCl_3$ solution]: L, 9.42(H(1), d, 5.5); 6.85 (H(2), t, 7.5); 7.99 (H(3), t, 8.1); 7.35 (H(4), d, 7.2); 6.40(H(6), s); 7.45–7.50 (H(8,9,11,12), m); 16.05 (NH_2, s); NC_6H_5, 7.09 (2H(o), d, 5.9); 7.13 (2H(m), t, 6.6); 7.19 (1H(p), t, 6.3).

1a: *Anal.* Calc. for $C_{18}H_{15}Cl_4N_4Re$: C, 35.12; H, 2.44; N, 9.10. Found: C, 35.17; H, 2.41; N, 9.06. UV–vis (λ_{max}, nm (ε, M^{-1} cm^{-1}), CH_2Cl_2 solution): 735 (1500); 540 (7600); 325 (13200). IR (cm^{-1}): 320, 335 (Re–Cl), 1595 (C=N). ^1H NMR [δ (*J*/Hz), $CDCl_3$ solution]: L, 9.39(H(1), d, 5.8); 6.83 (H(2), t, 7.5); 7.97 (H(3), t, 8.2); 7.34 (H(4), d, 7.4); 6.42(H(6), s); 7.44–7.53 (H(8,9,11,12), m); 16.06 (NH_2, s); NC_6H_4Cl, 7.05 (2H(o), d, 5.8); 7.12 (2H(m), d, 5.6).

4.2.2. Synthesis of $[Re^{VI}(NC_6H_4Y)Cl_3(C_{12}H_{10}N_3O)]$, **2**

The same general method was used to prepare the above complexes from $[Re^{V}(NC_6H_4Y)Cl_3(C_{12}H_{11}N_3)]$, **1**. Procedural details are given for one representative case (**2d**). Yields are in the range 75–80%.

One hundred and two milligrams (0.17 mmol) of **1d** was dissolved in 25 ml acetonitrile, and 4.5 ml 1(N) nitric acid (acidity ~0.15 N) was added. The violet solution was stirred for 1 h, during which the colour turned yellowish brown. Solvent evaporation yields dark brown product. The mass thus obtained was thoroughly washed with cold water to remove adherent nitric acid and finally dried in vacuum over fused $CaCl_2$. Yield: 80 mg (77%). *Anal.* Calc. for $C_{19}H_{17}Cl_3N_4O_2Re$: C, 36.45; H, 2.72; N, 8.95. Found: C, 36.40; H, 2.75; N, 8.99. UV–vis (λ_{max}, nm (ε, M^{-1} cm^{-1}), CH_2Cl_2 solution): 535 (1600); 355 (12200). IR (cm^{-1}): 320, 335 (Re–Cl), 1595 (C=N), 1635 (C=O).

2c: *Anal.* Calc. for $C_{19}H_{17}Cl_3N_4ORe$: C, 37.41; H, 2.79; N, 9.19. Found: C, 37.45; H, 2.75; N, 9.22. UV–vis (λ_{max}, nm (ε, M^{-1} cm^{-1}), CH_2Cl_2 solution): 535 (1600); 355 (12000). IR (cm^{-1}): 320, 335 (Re–Cl), 1595 (C=N), 1635 (C=O).

2b: *Anal.* Calc. for $C_{18}H_{15}Cl_3N_4ORe$: C, 36.27; H, 2.52; N, 9.40. Found: C, 36.30; H, 2.57; N, 9.33. UV–vis (λ_{max}, nm (ε, M^{-1} cm^{-1}), CH_2Cl_2 solution): 535 (1600); 355 (12300). IR (cm^{-1}): 325, 335 (Re–Cl), 1595 (C=N), 1635 (C=O).

2a: *Anal.* Calc. for $C_{18}H_{14}Cl_4N_4ORe$: C, 34.28; H, 2.22; N, 8.89. Found: C, 34.32; H, 2.25; N, 8.81. UV–vis (λ_{max}, nm (ε, M^{-1} cm^{-1}), CH_2Cl_2 solution): 535 (1500); 355 (12400). IR (cm^{-1}): 320, 330 (Re–Cl), 1595 (C=N), 1635 (C=O).

4.2.3. Synthesis of **1** from **2**

4.2.3.1. Hydrazine method. To a yellow–brown solution of **2** (125 mg, 0.20 mmol) in acetonitrile (25 ml) was added hydrazine sulphate (91 mg, 0.70 mmol) in 10 ml solvent. It was then stirred for 1.5 h at room temperature whereupon the solution gradually turned violet. The solvent was removed from the resulting solution under reduced pressure. The obtained violet mass (**1**) was washed with cold water to free adhered hydrazine and dried in vacuum over fused $CaCl_2$. Yield: 100 mg (82%).

4.2.3.2. Hydroxylamine method. To a yellow–brown solution of **2** (125 mg, 0.20 mmol) in acetonitrile (25 ml) was added hydroxylamine hydrochloride (28 mg, 0.40 mmol) in 5 ml solvent. It was then stirred for 8 h at room temperature. The solvent was removed from the resulting solution under reduced pressure. The obtained

Table 6
Crystallographic data for **1d**.

Complex	**1d**
Formula	$C_{19}H_{18}Cl_3N_4ORe$
M	610.92
System	monoclinic
Space group	P2(1)/c
a (Å)	9.123(2)
b (Å)	15.961(3)
c (Å)	15.333(3)
α (°)	90
β (°)	106.19(3)
γ (°)	90
V (Å^3)	2144.1(7)
Z	4
D (mg m^{-3})	1.893
T (K)	293(2)
μ (mm^{-1})	6.058
Independent reflections	5954
R_{int}	0.0410
Collected reflections	27807
*R*1, *wR*2 [$I > 2\sigma(I)$]	0.0251, 0.0516

violet mass (**1**) was washed with cold water to free adhered hydrazine and dried in vacuum over fused $CaCl_2$. Yield: 104 mg (84%).

*4.2.4. Synthesis of [Re^{V}OCl$_3$(C$_{12}$H$_{11}$N$_3$)], **6***

To a green solution of [$ReOCl_3(PPh_3)_2$] (208 mg, 0.25 mmol) in 30 ml of dichloromethane was added 60 mg (0.30 mmol) of L in 10 ml of dichloromethane, and the mixture was stirred for 20 min, affording a pink solution. The volume of the solvent was then reduced to one fifth under reduced pressure, and excess of n-hexane was added into it. It causes precipitation of the pink complex and the solution was then filtered. The pink product was collected by filtration and washed twice with diethyl ether. The mass was finally dried in vacuum over fused $CaCl_2$. The pink mass is unstable on silica gel column and can not be isolated by chromatography. Yield: 111 mg (88%). *Anal.* Calc. for $C_{12}H_{11}Cl_3N_3ORe$: C, 28.56; H, 2.18; N, 8.33. Found: C, 28.49; H, 2.24; N, 8.26. IR (cm^{-1}): 320, 335 (Re–Cl), 1595 (C=N), 998 (Re≡O).

4.3. X-ray crystallography

Dark violet single crystals of **1d** were obtained by slow diffusion of solvent pair (dichloromethane/hexane) at room temperature. Data were collected at $T = 293(2)$ K on a Siemens SMART CCD area-detector diffractometer equipped with graphite monochromated Mo Kα radiation ($\lambda = 0.71073$ Å, rotating anode source) in the range $1.88° = \theta = 30.55°$. All the data were corrected for Lorentz polarization and absorption [43]. The structure was generated by direct methods using SHELXS-97 [44] followed by successive Fourier synthesis and refined by full matrix least squares based on F^2 with SHELXL-97 [45]. Anisotropic displacement parameters were assigned to all non-hydrogen atoms. Significant crystal data are listed in Table 6. The crystallographic data have been deposited to CCDC.

Supplementary data

CCDC 673975 contains the supplementary crystallographic data for **1d**. These data can be obtained free of charge via http://www.ccdc.cam.ac.uk/conts/retrieving.html, or from the Cambridge Crystallographic Data Centre, 12 Union Road, Cambridge CB2 1EZ, UK; fax: (+44) 1223-336-033; or e-mail: deposit@ccdc.cam.ac.uk.

Acknowledgement

We thank the University Grants Commission (UGC), India for financial support.

References

[1] B.D. Sherry, A.T. Radosevich, F.D. Toste, J. Am. Chem. Soc. 125 (2003) 6076.
[2] E.A. Ison, E.R. Trived, R.A. Corbin, M.M. Abu-Omar, J. Am. Chem. Soc. 127 (2005) 15374.
[3] Y. Koninobu, Y. Nishina, C. Nakagawa, K. Takai, J. Am. Chem. Soc. 128 (2006) 12376.
[4] Y. Kuninobu, A. Kawata, K. Takai, J. Am. Chem. Soc. 127 (2005) 13498.
[5] M.M. Abu-Omar, E.H. Appelman, J.H. Espenson, Inorg. Chem. 35 (1996) 7751.
[6] E.A. Ison, J.E. Cessarich, G. Du, P.E. Fanwick, M.M. Abu-Omar, Inorg. Chem. 45 (2006) 2385.
[7] L.D. McPherson, M. Drees, S.I. Khan, T. Strassner, M.M. Abu-Omar, Inorg. Chem. 43 (2004) 4036.
[8] J.M. Mayer, Acc. Chem. Res. 31 (1998) 441.
[9] R.H. Holm, Chem. Rev. 87 (1987) 1401.
[10] D.E. Wigley, Prog. Inorg. Chem. 42 (1994) 239.
[11] J. Dixon, J.H. Espenson, Inorg. Chem. 41 (2002) 4727.
[12] Y. Wang, Inorg. Chem. 41 (2002) 2266.
[13] G. Lente, X. Shan, I.A. Guzei, J.H. Espenson, Inorg. Chem. 39 (2000) 3572.
[14] G. Lente, J.H. Espenson, Inorg. Chem. 39 (2000) 4197.
[15] B. Domereq, M. Fourmique, Eur. J. Inorg. Chem. 40 (2001) 1625.
[16] G.D.J. Correia, A. Domingos, I. Santos, Eur. J. Inorg. Chem. 39 (2000) 1523.
[17] P. Klufers, O. Krotz, M. Obberger, Eur. J. Inorg. Chem. 41 (2002) 1919.
[18] J.C. Bryan, R.E. Stenkemp, T.H. Tulip, J.M. Mayer, Inorg. Chem. 26 (1987) 2283.
[19] J. Gangopadhyay, S. Sengupta, S. Bhattacharyya, I. Chakraborty, A. Chakravorty, Inorg. Chem. 41 (2002) 2616.
[20] S. Sengupta, J. Gangopadhyay, A. Chakravorty, Dalton Trans. (2003) 4635.
[21] I. Chakraborty, S. Bhattacharyya, S. Banerjee, B.K. Dirghangi, A. Chakravorty, J. Chem. Soc., Dalton Trans. (1999) 3747.
[22] M.M. Abu-Omar, Chem. Commun. (2003) 2102.
[23] B.K. Dirghangi, M. Menon, S. Banerjee, A. Chakravorty, Inorg. Chem. 36 (1997) 3595.
[24] L.A. de Learie, R.C. Haltiwanger, C.G. Pierpont, Inorg. Chem. 26 (1987) 817.
[25] A. Abragam, B. Bleaney, Electron Paramagnetic Resonance of Transition Ions, Clarendon, Oxford, England, 1970.
[26] J. Baldas, J.F. Boas, J. Bonnyman, J.R. Pilbrow, G.A. Williams, J. Am. Chem. Soc. 107 (1985) 1886.
[27] J.F. Gibson, K. Mertis, G. Wilkinson, J. Chem. Soc., Dalton Trans. (1975) 1093.
[28] J.H. Holloway, J.B. Raynor, J. Chem. Soc., Dalton Trans. (1975) 737.
[29] U. Abram, M. Braun, S. Abram, R. Kirmse, A. Voigt, J. Chem. Soc., Dalton Trans. (1998) 231.
[30] W.A. Nugent, B.L. Haymore, Coord. Chem. Rev. 31 (1980) 123.
[31] G.V. Goeden, B.L. Haymore, Inorg. Chem. 22 (1983) 157.
[32] G. Lyashenko, V. Jancik, A. Pal, R.H. Irmev, N.C. Mosch-Zanetti, Dalton Trans. (2006) 1294.
[33] H. Taube, Electron Transfer Reactions of Complex Ions in Solution, New York, Academic Press, 1973.
[34] S. Pal, S. Pal, J. Chem. Soc., Dalton Trans. (2002) 2102.
[35] G. Bandoli, T.I.A. Gerber, R. Jacobs, J.G.H. Du Preez, Inorg. Chem. 33 (1994) 178.
[36] V. Katovic, S.C. Vergez, D.H. Busch, Inorg. Chem. 16 (1977) 1716.
[37] D.H. Busch, J.C. Bailer, J. Am. Chem. Soc. 78 (1956) 1137.
[38] C.M. Harris, E.D. Mckenzie, Nature 196 (1962) 670.
[39] L.A. Tyler, M.M. Olmstead, P.K. Mascharak, Inorg. Chem. 40 (2001) 5408.
[40] J. Chatt, J.D. Garforth, N.P. Johnson, G.A. Rowe, J. Chem. Soc. (1964) 1012.
[41] G.W. Parshall, Inorg. Synth. 17 (1977) 110.
[42] G. Bhar, H. Thamlitz, Z. Anorg. Allg. Chem. 282 (1955) 3.
[43] G.M. Sheldrick, SADABS, Absorption Correction Program, University of Gottingen,, Germany, 1996.
[44] G.M. Sheldrick, SHELXS-97, University of Gottingen, Germany, 1997.
[45] G.M. Sheldrick, SHELXL-97, University of Gottingen, Germany, 1997.